

INTERACTIONS OF MASSIVE STARS WITH THEIR PARENTAL CLOUDS

José Franco¹, Guillermo García-Segura¹ & Tomasz Plewa²

ABSTRACT

Here we discuss the interaction of massive stars with their parental molecular clouds. A summary of the dynamical evolution of HII regions and wind-driven bubbles in high-pressure cloud cores is given. Both ultracompact HII regions and ultracompact wind-driven bubbles can reach pressure equilibrium with their surrounding medium. The structures stall their expansion and become static and, as long as the ionization sources and the ambient densities remain about constant, the resulting regions are stable and long lived. For cases with negative density gradients, and depending on the density distribution, some regions never reach the static equilibrium condition. For power-law density stratifications, $\rho \propto r^{-w}$, the properties of the evolution depend on a critical exponent, w_{crit} , above which the ionization front cannot be slowed down by recombinations or new ionizations, and the cloud becomes fully ionized. This critical exponent is $w_{crit} = 3/2$ during the expansion phase. For $w > 3/2$ the gas expands supersonically into the surrounding ionized medium, and there are two regimes separated by $w = 3$. For $3/2 < w \leq 3$, the slow regime, the inner region drives a weak shock moving with almost constant velocity through the cloud. For $w > 3$, the fast regime, the shock becomes strong and accelerates with time. Finally, the evolution of slow winds in highly pressurized region is described briefly.

1. INTRODUCTION

Young stars display vigorous activity and their energy output stirs and heats the gas in their vicinity. Low-mass stars provide a small energy rate and affect only small volumes, but their collective action can provide partial support against the collapse of their parental clouds, and could regulate some aspects of the cloud evolution (*e.g.*, Norman & Silk 1980; Franco & Cox 1983; Franco 1984; McKee 1989). In contrast, stars with initial masses above $8 M_{\odot}$, massive stars, inject large amounts of radiative and mechanical energy from their moment of birth until their final explosion as a supernova. In the general, low-density, interstellar medium of a gaseous galaxy, the combined effects of supernovae, stellar winds, and HII region expansion destroy star-forming clouds, produce the hottest gas phases, create large expanding bubbles, and are probably responsible for both stimulating and shutting off the star formation process at different scales (*e.g.*, Cox & Smith 1974; Salpeter 1976; McKee & Ostriker 1977; Franco & Shore 1984; Cioffi & Shull 1991; Franco *et al.* 1994; Silich *et al.* 1996). Thus, the collection of OB associations in gaseous galaxies represents a rich energy source which may be controlling the general structure of the interstellar medium, and the star formation rate (*e.g.*, Mueller & Arnett 1976; Gerola & Seiden 1978; Franco & Shore 1984; Dopita 1988; see reviews by Tenorio-Tagle & Bodenheimer 1988, Franco 1991,1992, Ferrini 1992, and Shore & Ferrini 1994).

The strong UV radiation field from massive stars create large photoionized, HII regions. Young HII regions have large pressures and, when the pressure of the surrounding medium is low, they expand fast and drive a strong shock wave ahead of the ionization front. Expanding HII regions ionize and stir the parental cloud and, when the ionization front encounters a strong negative density gradient, they create fast “champagne” flows and can also generate cometary globules and elephant trunks (*e.g.*, Tenorio-Tagle 1982; Yorke 1986; Franco *et al.* 1989,1990; Rodriguez-Gaspar *et al.* 1995; García-Segura & Franco 1996). These flows are generated by the pressure difference between the HII region and the ambient medium, and they are responsible for the disruption of the cloud environment (*e.g.*, Whitworth 1979; Elmegreen 1983; Larson 1992; Franco *et al.* 1994). Individual HII regions are bright objects and they are used as tracers of the active star formation sites in external galaxies (*e.g.*, Osterbrock 1989).

¹Instituto de Astronomía-UNAM, Apdo. Postal 70-264, 04510 México D. F., México

²Max-Planck-Institut für Astrophysik, Garching, Germany

Stellar winds and supernova explosions, on the other hand, being powerful sources of mechanical energy generate overpressured regions which drive shock waves into the ambient medium (see reviews by Ostriker & McKee 1988, and Bisnovatyi-Kogan & Silich 1995). The resulting wind-driven bubbles and supernova remnants, either from a single progenitor or from an entire association, are believed to generate most of the structuring observed in a gaseous galactic disk (*e.g.*, Reynolds & Ogden 1978; Cowie *et al.* 1979; Heiles 1979; McCray & Snow 1979). Actually, many observed structures in the Milky Way and in external galaxies have been ascribed to this stellar energy injection (*e.g.*, Heiles 1979, 1984; Brinks & Bajaja 1986; Deul & Hartog 1990; Palous *et al.* 1990, 1994). These bubbles may create fountains or winds at galactic scales (*e.g.*, Shapiro & Field 1976; Chevalier & Oegerle 1979; Bregman 1980; Cox 1981; Heiles 1990; Houck & Bregman 1990), and their expanding shocks have also been suspected of inducing star formation (*e.g.*, Herbst & Assousa 1977; Dopita *et al.* 1985). Thus, stellar activity creates a collection of cavities with different sizes, and can be viewed as an important element in defining the structure and activity of star-forming galaxies. Galaxies, however, are open systems and their properties are also defined by the interactions with neighboring galaxies. Here we describe only the effects of the stellar energy injection in high-density, high-pressure, regions.

2. THE PARENTAL CLOUDS AND MASSIVE STARS

Molecular clouds have complex density and velocity distributions, and are composed of a variety of high-density condensations. In our Galaxy, they have non-thermal turbulent velocities, reaching up to about 10 km s^{-1} , and fairly strong magnetic fields, of up to tens of mG (*e.g.*, Myers & Goodman 1988). The *average* densities for molecular cloud complexes is between 10^2 and 10^3 cm^{-3} , but the high-density condensations have average densities of about $\sim 10^6 \text{ cm}^{-3}$ and may even reach values in excess of 10^8 cm^{-3} (*e.g.*, Bergin *et al.* 1996; Akeson *et al.* 1996; see review by Walmsley 1995). These high density condensations, or cloud cores, are the actual sites of star formation, and the initial shape and early evolution of the resulting HII regions depend on the corresponding core density distributions and pressures. Theoretical studies on the collapse of clouds indicate that rotating and magnetized cores evolve into flattened (disk-like) structures (*e.g.*, Bodenheimer & Black 1978; Cassen *et al.* 1985), but nonrotating and nonmagnetic cases remain spherically symmetric with power-law density distributions (*e.g.*, Larson 1974). Isothermal spheres in hydrostatic equilibrium have a density distribution $\rho \sim r^{-2}$, and the distribution evolves towards $r^{-3/2}$ during the free-fall collapse. The pressures at the centers of these cores are fairly large, and can reach values of about 5 or 6 orders of magnitude above the pressures at the cloud boundaries (see García-Segura & Franco 1996).

Recent observational studies are revealing the structure of the dense star forming regions (see review by Walmsley 1995), and provide the average parameters of the core density distributions. Radio observations of cloud cores and dark clouds, along with visual extinction studies in nearby star forming clouds, indicate internal density distributions ranging from r^{-1} to r^{-3} (*e.g.*, Arquilla & Goldsmith 1985; Chemicaro *et al.* 1985; Gregorio Hetem *et al.* 1988; see also Myers 1985). A reasonable mean value for the observationally derived power-law distributions is $\rho \sim r^{-2}$. The typical sizes of the massive high-density cores are about $r_c \sim 0.1 \text{ pc}$ (see Walmsley 1995), and the observationally derived core masses are in the range of 10 to $300 M_\odot$ (*e.g.*, Snell *et al.* 1993). The observed properties of ultracompact HII regions (UCHII), on the other hand, indicate that the exciting stars (one or several massive stars) are embedded in dense and warm cores, with densities between 10^4 - 10^7 cm^{-3} and temperatures of about 10^2 K (*e.g.*, Churchwell 1990; Cesaroni *et al.* 1994; Kurtz *et al.* 1994; Hofner *et al.* 1996; Hurt *et al.* 1996). The early stages of HII region evolution, then, occur inside these dense cloud cores.

2.1. HII region expansion at constant densities

Beginning with Strömgren (1939) and Kahn (1954), the expansion and evolution of HII regions has been studied with analytical and numerical models (see Yorke 1986; Osterbrock 1989; Franco *et al.* 1989,1990). For a constant photon flux and uniform ambient densities, the evolution has well defined formation and expansion phases. During the formation phase, the UV photon field creates an ionization front that moves through the gas. Its speed is reduced (by geometrical dilution and recombinations), approaching a value of about twice the speed of sound in the ionized gas in, approximately, one recombination time. At this moment, which marks the end of the formation phase, the HII region reaches the initial Strömgren size, and the pressure gradient across the ionization front begins to drive the expansion of the ionized gas. The expansion is supersonic with respect to the surrounding gas and creates a shock wave that accelerates and compresses the ambient shocked medium. The ionization front sits behind the shock front during the rest of the evolution, and most of the shocked gas is accumulated in the interphase between the two fronts. If either the ionization or the shock front encounters

a strong negative density gradient (say, the edge of the cloud) and overruns it, then the HII region enters into its champagne phase. Numerical models indicate that there also appears a strong instability that can fragment the shocked shell, and may explain the existence of cometary globules and the highly irregular morphologies of ionized nebulae (see García-Segura & Franco 1996).

2.1.1. The Formation Phase

Assuming a self-gravitating spherical cloud with a molecular density distribution that includes a central core, with radius r_c and constant density n_c , and an isothermal envelope with a power-law density stratification $n_{H_2}(r) = n_c(r/r_c)^{-2}$ for $r \geq r_c$. The total pressure at the core center is

$$P(0) = P_0 = \frac{2\pi G}{3}\rho_c^2 r_c^2 + P(r_c) = \frac{8}{5}P(r_c) \simeq 2 \times 10^{-7} n_6^2 r_{0.1}^2 \quad \text{dyn cm}^{-2}, \quad (1)$$

where G is the gravitational constant, $P(r_c)$ is the pressure at the core boundary $r = r_c$, $n_6 = n_c/10^6 \text{ cm}^{-3}$, and $r_{0.1} = r_c/0.1 \text{ pc}$. Note that the corresponding molecular mass is

$$M_c \simeq \left(\frac{\pi P_0}{G}\right)^{1/2} r_c^2 \sim 10^2 P_7^{1/2} r_{0.1}^2 \quad M_\odot, \quad (2)$$

where $P_7 = P_0/10^{-7} \text{ dyn cm}^{-2}$. A star located at the cloud center and producing F_* ionizing photons per unit time creates an spherical HII region. The gas in the HII region is fully ionized and the ion density is simply twice the molecular density, $n_i = 2n_{H_2}$. The initial Strömgen radius generated by such a star is

$$R_s = \left[\frac{3 F_*}{4\pi(2n_c)^2\alpha_B}\right]^{1/3} \simeq 2 \times 10^{-3} F_{48}^{1/3} n_6^{-2/3} \alpha_0^{-1/3} \text{ pc}, \quad (3)$$

where α_B is the hydrogen recombination coefficient to all levels above the ground level, $\alpha_0 = \alpha_B/2.6 \times 10^{-13} \text{ cm}^3 \text{ s}^{-1}$, $F_{48} = F_*/10^{48} \text{ s}^{-1}$, and $n_6 = n_c/10^6 \text{ cm}^{-3}$. Thus, $R_s < r_c$ and the initial HII region is well contained within the core, and the formation phase follows the well known constant density evolution described above. Note that for a dusty cloud, the initial radius is even smaller and is given by the transcendental equation $R_{S,\text{dust}} \simeq R_S e^{-\tau/3}$ (Franco *et al.* 1990), where the optical depth due to dust absorption is $\tau = \int_0^{R_{S,\text{dust}}} \sigma_{\text{dust}} n_0 dr$, and σ_{dust} is the average dust absorption cross-section per gas particle. This approximation agrees to better than 10% with detailed radiative transfer calculations (Díaz *et al.* 1996).

The formation phase is completed in a recombination time, and the pressure in the ionized region drives a shock into the molecular ambient medium. The HII region now begins its expansion phase. The equilibrium temperature in the photoionized region, $T_i \sim 10^4$, is achieved in a relatively short time scale. The advance of the ionization front is controlled by recombinations in the photoionized gas, and the expansion proceeds in a nearly isothermal fashion. Neglecting the external pressure, the main features of the expansion in a constant density medium can be derived with the thin shell approximation (see reviews Ostriker & McKee 1988, Bisnovaty-Kogan & Silich 1995, and García-Segura & Franco 1996). Also, the pressureless expansion in density stratifications can be solved with simple approximations to the shock front conditions (Franco *et al.* 1989,1990). The evolution including the external pressure, however, cannot be solved in a closed analytical form, but one can derive limits to the main expected features. Obviously, detailed numerical simulations provide an adequate description of the evolution in this and more complicated cases.

2.1.2. The Expansion Phase

The evolution can be easily derived by assuming the existence of a thin shell with mass M , containing all the swept-up ambient gas. This approximation can be applied to HII regions when the fraction of mass eroded by the ionization front from the shell is small. This is true for constant, increasing, or mildly decreasing density stratifications, but is not applicable for strongly decreasing gradients because the shell is easily eroded by photoionization (Franco *et al.* 1990). Here we consider the constant density case and the thin shell approximation can be used without restrictions. Neglecting magnetic fields and self-gravity, the equation of motion of the shell, located at a distant R from the central star, is

$$4\pi R^2(P_i - P_0) = \frac{d}{dt}(Mv), \quad (4)$$

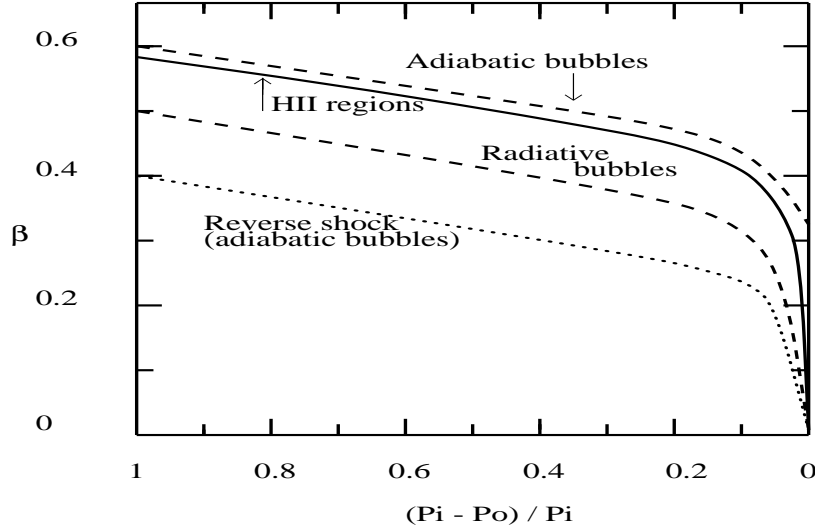


Fig. 1. The evolution of the exponent β as a function of the normalized pressure difference $(P_i - P_0)/P_i$.

where P_i is the internal pressure, P_0 is the external pressure, and v is the shell velocity. Assuming that the shell radius can be written as a power-law in time, $R = R_0 \zeta^\beta$ (where R_0 is the initial radius of the region, $\zeta = (t_0 + t)/t_0$, and t_0 is a reference initial time), with constant R_0 or β (*i.e.*, neglecting the existence of terms with \dot{R}_0 and $\dot{\beta}$), the right hand side of the equation becomes

$$\frac{d}{dt}(Mv) = \left(\frac{4\beta - 1}{3\beta}\right) 4\pi\rho_0 R^2 v^2. \quad (5)$$

The assumption of a constant β , as we will see below, does not hold for cases with $P_0 > 0$, but the present approximations can still be applied in a piece-wise fashion (*i.e.*, one can use them in segments, changing the values for R_0 and t_0).

The equation of motion can then be written as

$$P_i - P_0 = \rho_0 v^2 \frac{(4\beta - 1)}{3\beta}, \quad (6)$$

and the shell evolution is given by

$$\frac{dR}{dt} = \left[\frac{3\beta}{(4\beta - 1)} \frac{(P_i - P_0)}{\rho_0} \right]^{1/2}. \quad (7)$$

Thus, one can write the formal solution to the equation of motion simply as

$$R - R_0 = \int_1^\zeta \left[\frac{3\beta}{(4\beta - 1)\rho_0} (P_i - P_0) \right]^{1/2} t_0 d\zeta. \quad (8)$$

This formal solution can be applied to HII regions, wind-driven bubbles, and SN remnants (see below). Obviously, the integration is not straightforward unless $P_0 = 0$, or the pressure difference, $P_i - P_0$, can be written as an explicit function of either R or t . In general this is not possible, but one can *always* check the behavior at early and late times, when the external pressure can be neglected and when the internal and external pressures become comparable. Here we illustrate the behavior in both cases.

2.1.3. Pressure Equilibrium

For the case of expanding HII regions, using $R_0 = R_S$ as the initial Strömngren radius, we can set the solution for the expansion simply as

$$R_{HII}(t) = R_S \zeta^\beta. \quad (9)$$

The average ion density inside the HII region at any given time is given by

$$\langle n_i \rangle = \left[\frac{3 F_\star}{4 \pi \alpha_B} \right]^{1/2} R_{HII}^{-3/2}, \quad (10)$$

and the corresponding internal pressure is

$$P_i = \left(\frac{3 k^2 T_i^2 F_\star}{\pi \alpha_B} \right)^{1/2} R_{HII}^{-3/2}. \quad (11)$$

The region, then, evolves as

$$R_{HII} = R_S + \int_1^\zeta \left(\frac{3\beta}{(4\beta-1)\rho_0} \left[\left(\frac{3 k^2 T_i^2 F_\star}{\pi \alpha_B R_S^3 \zeta^{3\beta}} \right)^{1/2} - P_0 \right] \right)^{1/2} t_0 d\zeta. \quad (12)$$

At early times, when $P_0/P_i \ll 1$, the integration with constant β gives $R_{HII} \propto \zeta^{1-3\beta/4}$. Thus, our initial assumption for the power-law implies that $\beta = 1 - 3\beta/4$, and one gets $\beta = 4/7$. The solution, then, is now written as

$$R_{HII} = R_S \left[1 + \frac{7}{4} \left(\frac{8 k T_i}{3 \mu_H} \right)^{1/2} \frac{t_0}{R_S} (\zeta^{4/7} - 1) \right]. \quad (13)$$

Defining $c_i \simeq (8 k T_i / 3 \mu_H)^{1/2}$, and recalling the initial definition of the power-law $\zeta^{4/7} = R_{HII}/R_S$, the reference time is simply given by $t_0 = (4/7)(R_S/c_i)$. Thus, as expected, one recovers the well known law for HII region expansion in a pressureless medium with a constant density

$$R_{HII} \simeq R_S \left(1 + \frac{7 c_i t}{4 R_S} \right)^{4/7}. \quad (14)$$

Using this explicit time dependence, the internal pressure decreases as

$$P_i = P_{i,0} \left(1 + \frac{7 c_i t}{4 R_S} \right)^{-6/7}, \quad (15)$$

where $P_{i,0}$ is the pressure at $t = 0$.

The expansion continues until $P_i \rightarrow P_0$, and the internal pressure tends to a constant value. In this limit, the time dependence in the formal solution vanishes, giving $3\beta/2 \rightarrow 0$. These limits show that, for a constant density medium, β evolves as a function of the pressure difference from $4/7$ to zero. Figure 1 shows the evolution of β , as a function of the normalized pressure difference $(P_i - P_0)/P_i$, for HII regions and wind-driven bubbles (García-Segura & Franco 1996). The exponents were derived from high-resolution numerical simulations performed in one dimension for the evolution inside high density cores. Figure 2 shows the evolution of an HII region in a high-density core with $P_7 = 1$.

When pressure equilibrium is reached, the ion density is simply given by

$$n_{i,\text{eq}} = \left(\frac{P_0}{2kT_i} \right) \simeq 3.6 \times 10^4 P_7 T_{\text{HII},4}^{-1} \text{ cm}^{-3}, \quad (16)$$

where $P_7 = P_0/10^{-7} \text{ dyn cm}^{-2}$, and $T_{\text{HII},4} = T_i/10^4 \text{ K}$. The equilibrium radius of the H II region, then, corresponds to a Strömgen radius at this equilibrium density

$$R_{\text{S,eq}} \approx 2.9 \times 10^{-2} F_{48}^{1/3} T_{\text{HII},4}^{2/3} P_7^{-2/3} \text{ pc}, \quad (17)$$

where $F_{48} = F_\star/10^{48} \text{ s}^{-1}$.

For high-pressure cores with $r_c \sim 0.1 \text{ pc}$, the photoionized regions can reach pressure equilibrium without breaking out of the core. The resulting sizes are similar to those of the ultracompact class (see Dyson *et al.* in

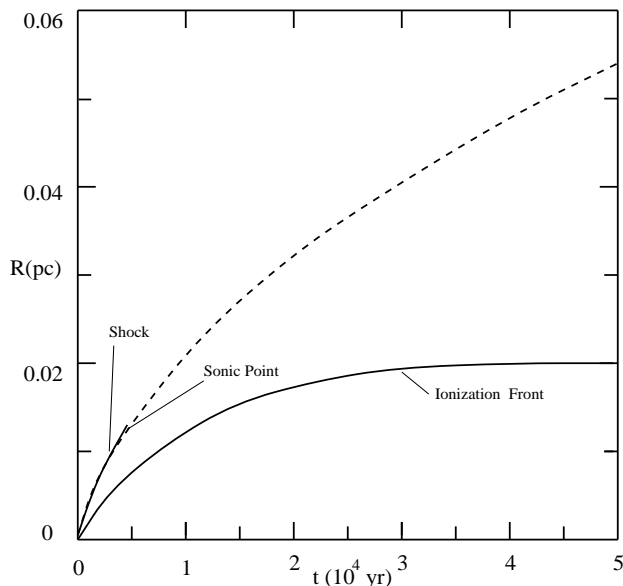


Fig. 2. The evolution of an HII region, with $F_{48} = 1$, in a high-pressure core, with $P_7 = 1$.

this volume), and indicate that UCHII can be explained by simple pressure equilibrium. This is in agreement with the recent results reported by Xie *et al.* (1996), that show the smaller UCHII are embedded in the higher pressure cores. Also note that the equilibrium values with $P_7 = 1$, $T_{\text{HII},4} \sim 1$, and $F_{48} \sim 1$, are *very similar* to the average sizes and electron densities in UCHII (see Figure 151 of Kurtz *et al.* 1994). The apparent longevity problem of UCHIIs is rooted in the notion that young HII regions should grow fast and reach the expanded state on a relatively short time-scale. This statement is false, however, if the external pressure is large and halts the expansion at a small radius: *in pressure equilibrium, UCHIIs are stable and long lived.*

2.2. HII Evolution in Decreasing Density Gradients

If a star is born at a distance smaller than $R_{S,\text{eq}}$ from the core boundary, the speeds of the ionization and shock fronts are modified by the negative density gradient. The gas of the HII regions is accelerated in supersonic flows and no static solution, in pressure equilibrium exists (*e.g.*, Tenorio-Tagle 1982; Franco *et al.* 1989, 1990). Thus, under these conditions the ultracompact stage is indeed a transient phase. Here we assume isothermal clouds with $\rho \propto r^{-2}$, but one can easily find the solutions for the general power-law case, $\rho \propto r^{-w}$ (see Franco *et al.* 1990). For $R_s \geq r_c$, the initial ionization front reaches the core radius with a speed

$$U_c \simeq 90 \alpha_0 n_3 r_{17} \left[\left(\frac{R_s}{r_c} \right)^3 - 1 \right] \text{ km s}^{-1}, \quad (18)$$

and in a time scale

$$t_c \simeq 130 \alpha_0^{-1} n_3^{-1} \ln \left[\frac{1}{1 - (r_c/R_s)^3} \right] \text{ yr}, \quad (19)$$

where $r_{17} = r_c/10^{17}$ cm. Afterwards, the ionization front enters the density gradient and its speed becomes

$$U_{if} = \frac{U_c}{(R_s/r_c)^3 - 1} u(w), \quad (20)$$

with

$$u(w) = \begin{cases} (r_c/r_i)^{2-w} \left[(R_s/r_c)^3 + 2w\beta - 3\beta (r_i/r_c)^{1/\beta} \right] & \text{for } w \neq 3/2, \\ (r_c/r_i)^{1/2} \left[(R_s/r_c)^3 - 1 - 3 \ln (r_i/r_c) \right] & \text{for } w = 3/2, \end{cases} \quad (21)$$

where r_i is the location of the front, and $\beta = (3 - 2w)^{-1}$. This defines a critical exponent, corresponding to the maximum density gradient that is able to stop the ionization front,

$$w_f = \frac{3}{2} \left[1 - \left(\frac{r_c}{R_s} \right)^3 \right]^{-1}, \quad (22)$$

and above which no initial HII radius exists. Note that for $R_s/r_c > 2$ the critical value becomes $w_f \simeq 3/2$. Obviously, the concept of a critical exponent is not restricted to power-law stratifications and can also be applied to other types of density distributions, for instance, exponential, gaussian, and sech² profiles (see Franco *et al.* 1989).

For $w \neq 3/2$, the initial HII region radius can be written as

$$R_w = g(w)R_s, \quad (23)$$

with

$$g(w) = \left[\frac{3 - 2w}{3} + \frac{2w}{3} \left(\frac{r_c}{R_s} \right)^3 \right]^\beta \left(\frac{R_s}{r_c} \right)^{2w\beta}, \quad (24)$$

where R_s is the Strömgen radius for the density n_c . The solution for $w = 3/2$ is

$$R_{3/2} = r_c \exp \left\{ \frac{1}{3} \left[\left(\frac{R_s}{r_c} \right)^3 - 1 \right] \right\}. \quad (25)$$

After the formation phase has been completed in clouds with $w \leq w_f$, the HII region begins its expansion phase. For simplicity, we assume that the shock evolution starts at $t = 0$ when R_w is achieved. Given that the expansion is subsonic with respect to the ionized gas, the density structure inside the HII region can be regarded as uniform and its average ion density at time t is

$$\rho_i(t) \simeq \mu_i \frac{(9 - 6w)^{1/2}}{3 - w} (2n_c) R_s^{3/2} R^{-3/2}(t), \quad (26)$$

where μ_i is the mass per ion, and $R(t)$ is the radius of the HII region at the time t . For $w \leq 3/2$, the radius can be approximated by

$$R(t) \simeq R_w \left[1 + \frac{7 - 2w}{4} \left(\frac{12}{9 - 4w} \right)^{1/2} \frac{c_i t}{R_w} \right]^{4/(7-2w)}, \quad (27)$$

where c_i is the sound speed in the ionized gas. The ratio of total mass (neutral plus ionized), $M_s(t)$, to ionized mass, $M_i(t)$, contained within the expanded radius evolves as

$$\frac{M_s(t)}{M_i(t)} \simeq \left[\frac{R(t)}{R_w} \right]^{(3-2w)/2}. \quad (28)$$

This equation indicates: i) for $w < 3/2$, the interphase between the ionization front and the leading shock accumulates neutral gas and its mass grows with time to exceed even the mass of ionized gas, and ii) for $w = 3/2 = w_{crit}$, the two fronts move together without allowing the formation and growth of a neutral interphase. Note that the decreasing ratio predicted by equation (28) for $w > 3/2$ is physically meaningless and it only indicates that the ionization front overtakes the shock front (and proceeds to ionize the whole cloud). Thus, regardless of the value of the critical exponent for the formation phase, w_f , the expansion phase is characterized by a critical exponent with a well defined value, $w_{crit} = 3/2$, which is independent of the initial conditions. Furthermore, this critical exponent $w_{crit} = 3/2$ is not affected by dust absorption (see Franco *et al.* 1990).

For $3/2 < w < w_f$, the ionization front overtakes the shock and the whole cloud becomes ionized. In this case, the pressure gradient simply follows the density gradient. The ionized cloud is set into motion, but the expanded core (now with a radius identical to the position of the overtaken shock) is the densest region and feels the strongest outwards acceleration. Then, superimposed on the general gas expansion there is a wave driven by the fast growing core (the wave location defines the size of the expanded core), and the cloud

experiences the so-called “champagne” phase. This core expansion tends to accelerate with time and two different regimes, separated by $w = 3$, are apparent: a *slow* regime with almost constant expansion velocities, and a *fast* regime with strongly accelerating shocks. The slow regime corresponds to $3/2 < w < 3$ and the core grows approximately as

$$r(t) \simeq r_c + \left[1 + \left(\frac{3}{3-w} \right)^{1/2} \right] c_i t, \quad (29)$$

where for simplicity the initial radius of the denser part of the cloud has been set equal to r_c , the initial size of the core. For $w = 3$ the isothermal growth is approximated by

$$r(t) \simeq 3.2 r_c \left[\frac{c_i t}{r_c} \right]^{1.1}. \quad (30)$$

For $w > 3$, the fast regime, the shock acceleration increases with increasing values of the exponent and the core expansion is approximated by

$$r(t) \simeq r_c \left[1 + \left(\frac{4}{w-3} \right)^{1/2} \left(\frac{\delta+2-w}{2} \right) \frac{c_i t}{r_c} \right]^{2/(\delta+2-w)}, \quad (31)$$

where $\delta \simeq 0.55(w-3) + 2.8$.

2.3. Wind-driven Bubbles

The evolution of the cavity created by a stellar wind, a wind-driven bubble, can also be derived with the thin shell approximation described above. The thermalization of the wind creates a hot shocked region enclosed by two shocks: a reverse shock that stops the supersonic wind, and an outer shock that penetrates the ambient gas. The gas processed by each shock is separated by a contact surface, the contact discontinuity. The kinetic energy of the wind is transformed into thermal energy at the reverse shock producing a hot gas (*e.g.*, Weaver *et al.* 1977). For the case of a strong wind evolving in a high-density and dusty molecular core, the properties of the cooling are poorly known, but the shocked ambient gas cools down very quickly and a thin external shell is formed on time-scales of the order of years. Thus, the ambient gas is collected in a thin shell by the outer shock during most of the evolution. The case of the shocked stellar wind is less clear because the cooling time there can be substantially longer than in the shocked ambient gas, and it is difficult to define when the thin shell is formed behind the reverse shock. Thus, one can simply derive the limits for the evolution of the reverse shock in both the adiabatic and radiative modes.

The density in a steady wind, with a constant mass loss, decreases as

$$\rho_w = \frac{\dot{M}}{4\pi r^2 v_\infty}, \quad (32)$$

where \dot{M} is the stellar mass-loss rate, and v_∞ is the wind speed. The pressure in the shocked wind region is defined by the wind ram pressure, $\rho_w v_\infty^2$, at the location of the reverse shock and is given by

$$P_i = \frac{\dot{M} v_\infty}{4\pi R_{rs}^2}, \quad (33)$$

where R_{rs} is the radius of the reverse shock.

2.3.1. Adiabatic Case

For an adiabatic bubble evolving in a constant density medium and powered by a constant mechanical luminosity, L_w , the thermal energy of the shocked wind region grows linearly with time, $E_{th} = 5 L_w t / 11$ (Weaver *et al.* 1977). The shocked ambient medium is concentrated in the external thin shell and the bubble radius, R_b is the radius of the contact discontinuity. The thermal pressure of the bubble interior changes

as $P_i = (5L_w t)/(22\pi R_b^3)$. This pressure is equal to that given by equation (33), and the locations of the reverse and outer shocks are related by mass conservation

$$R_{rs} = R_b^{3/2} \left(\frac{11\dot{M}v_\infty}{10L_w t} \right)^{1/2}. \quad (34)$$

The solution for R_b , then, also provides the evolution of the reverse shock. The initial radius in this case is very small, and we simply set $R_b = R_0(t/t_0)^\beta$, where R_0 now represents the bubble radius at some reference time t_0 . Again, as in the HII region case, the formal solution is

$$R_b = \int_0^t \left[\frac{3\beta}{(4\beta - 1)\rho_0} \left(\frac{5L_w t^{1-3\beta} t_0^{3\beta}}{22\pi R_0^3} - P_0 \right) \right]^{1/2} dt. \quad (35)$$

At early times, $P_i \gg P_0$ and P_0 can be neglected in the above equation. The exponent is then defined by $\beta = 1 + (1 - 3\beta)/2$, giving the well known adiabatic expansion in a medium with constant density $R_b \propto L_w^{1/5} \rho_0^{-1/5} t^{3/5}$. The position of the reverse shock (equation 34), then, evolves as $R_{rs} \propto t^{2/5}$. With this time dependence, the internal pressure drops as $P_i \propto t^{-4/5}$. At later times, when $P_i \rightarrow P_0$, the bubble reaches quasi-equilibrium with the ambient gas and the growth is $R_{b,\text{eq}} \propto (L_w/P_0)^{1/3} t^{1/3}$. In pressure equilibrium, the radius of an *adiabatic* bubble grows at a slow rate, but *no steady state* solution exists during this stage. The final radius of the reverse shock is simply given by the balance between the external and the wind ram pressures. The wind density at equilibrium is $\rho_{w,\text{eq}} = P_0/v_\infty^2$, and the location of the reverse shock is

$$R_{rs,\text{eq}} = \left[\frac{\dot{M} v_\infty}{4\pi P_0} \right]^{1/2} \simeq 2.3 \times 10^{-2} \left[\frac{\dot{M}_6 v_{\infty,8}}{P_7} \right]^{1/2} \text{ pc}, \quad (36)$$

where $\dot{M}_6 = \dot{M}/10^{-6} M_\odot \text{ yr}^{-1}$, and $v_{\infty,8} = v_\infty/10^8 \text{ cm s}^{-1}$. Using mass conservation in the shocked wind region, $M_{sw} = \dot{M}t$, the quasi-equilibrium radius of an *ultracompact* wind-driven bubble is given by

$$R_{b,\text{eq}} = R_{rs,\text{eq}} \left(1 + \frac{3L_w t}{8\pi P_0 R_{rs,\text{eq}}^3} \right)^{1/3}. \quad (37)$$

Clearly, for adiabatic bubbles, β goes from $3/5$ at early times to $1/3$ at late times.

2.3.2. Radiative Case

Once radiative losses become important, the hot gas loses its pressure and the bubble collapses into a simple structure: the free-expanding wind collides with the cold shell and the gas is thermalized and cools down to low temperatures in a cooling length. At this moment, the shell becomes static at the radius $R_{rs,\text{eq}}$.

If the bubble becomes radiative before the final radius, $R_{rs,\text{eq}}$, is reached, the shell is pushed directly by the wind pressure. For this radiative bubble case, the formal solution is

$$R_b = \int_0^t \left[\frac{3\beta}{(4\beta - 1)\rho_0} \left(\frac{\dot{M} v_\infty t_0^{2\beta}}{4\pi R_0^2 t^{2\beta}} - P_0 \right) \right]^{1/2} dt. \quad (38)$$

The early times solution, with $P_i \gg P_0$, gives the relation $\beta = 1 - \beta$, and one recovers the well known solution for radiative bubbles $R_b \propto t^{1/2}$ (*e.g.*, Steigman *et al.* 1975). The ram pressure now evolves as $P_i \propto t^{-1}$. At late times, one gets $\beta \rightarrow 0$ and the shell reaches the final equilibrium radius (eqn. 36). Thus, the exponent in this case evolves from $1/2$ to 0 . Note that if the bubble starts on an adiabatic track and becomes radiative before pressure equilibrium is achieved, the exponent varies from $3/5$ to $1/2$, and then to zero. Figure 3 illustrates the evolution of an ultracompact wind-driven shell in a high-pressure core.

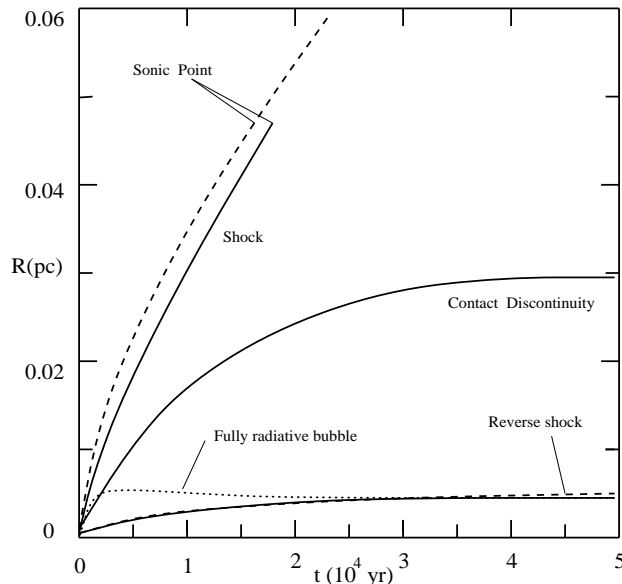


Fig. 3. The evolution of an ultracompact wind-driven bubble, with $\dot{M}_6 = 1$ and $v_{\infty,8} = 1$, in a high-pressure core, with $P_7 = 1$.

3. DISCUSSION

3.1. Young Stars

The history of the pressure in a star forming region, then, follows a somehow simple scheme. The initial properties and pressure of the gas in a star forming cloud is defined by self-gravity. Once young stars appear, their energy input modifies the structure and evolution of the cloud. This is particularly true for massive stars, their radiative and mechanical energy inputs are even able to disrupt their parental clouds. In the case of the dense cloud cores, the sizes of either HII regions or wind-driven bubbles are severely reduced by the large ambient pressure (García-Segura & Franco 1996). In fact, the pressure equilibrium radii of ultra-compact HII regions are actually indistinguishable from those of ultra-compact wind-driven bubbles, and they could be stable and long lived. Actually, Xie *et al.* (1996) have recently found evidence indicating that the smaller UCHII seem to be embedded in the higher pressure cores.

The situation is completely different when the stars are located near the edge of the cloud core. The resulting HII regions (and also wind-driven bubbles) generate supersonic outflows. Cases with $w > w_{crit}$ lead to the champagne phase: once the cloud is fully ionized, the expansion becomes supersonic. For spherical clouds with a small constant-density core and a power-law density distribution, r^{-w} , outside the core, there is a critical exponent ($w_{crit} = 3/2$) above which the cloud becomes completely ionized. This represents an efficient mechanism for cloud destruction and, once the parental molecular cloud is completely ionized, can limit the number of massive stars and the star formation rate (Franco *et al.* 1994). For a cloud of mass M_{GMC} , with only 10% of this mass concentrated in star-forming dense cores, the number of newly formed OB stars required for complete cloud destruction is

$$N_{OB} \sim 30 \frac{M_{GMC,5} n_3^{1/5}}{F_{48}^{3/5} (c_{i,15} t_{MS,7})^{6/5}}. \quad (39)$$

where $M_{GMC,5} = M_c/10^5 M_\odot$, $n_3 = n_0/10^3 \text{ cm}^{-3}$, $c_{i,15} = c_i/15 \text{ km s}^{-1}$, and $t_{MS,7}$ is the main sequence lifetime in units of 10^7 yr . This corresponds to a total star forming efficiency of about $\sim 5 \%$ (larger average densities and cloud masses can result in higher star formation efficiencies).

Summarizing, photoionization from OB stars can destroy the parental cloud in relatively short time scales, and defines the limiting number of newly formed stars. The fastest and most effective destruction mechanism is due to peripheral, blister, HII regions, and they can limit the star forming efficiency at galactic scales. Internal HII regions at high cloud pressures, on the other hand, result in large star forming efficiencies and they may be the main limiting mechanism in star forming bursts and at early galactic evolutionary stages (see Cox 1983).

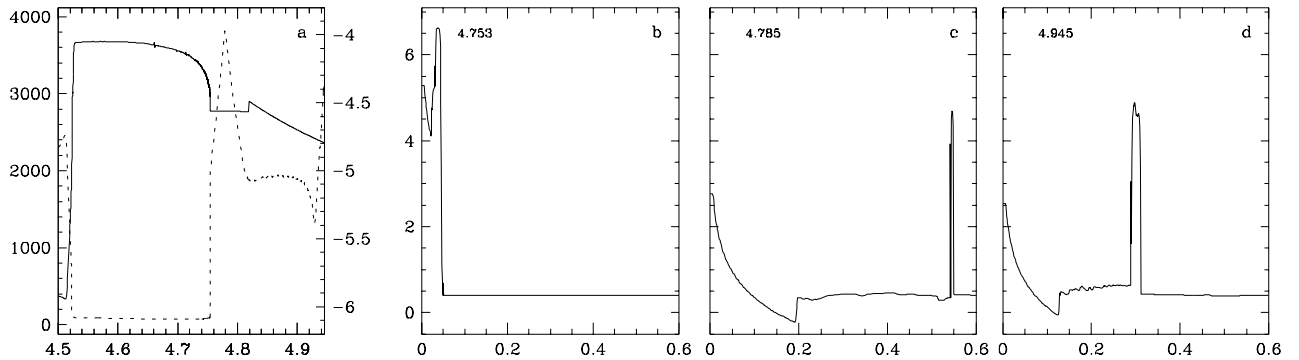


Fig. 4. Wind-driven bubble from an evolved $35 M_{\odot}$ star in a high pressure medium. **a)** Left scale: terminal wind velocity (km s^{-1}); right scale: mass loss rate ($M_{\odot} \text{ yr}^{-1}$); horizontal scale: time (millions of yr). **(b)-(d):** Evolution of the wind-driven bubble. The gas density (cm^{-3}) is plotted in a logarithmic scale versus the radial distance (pc). Evolutionary times (upper-left corner of each panel) are given in million years.

3.2. Slow Winds from Evolved Stars

The evolution of evolved stellar winds in high-pressure regions is discussed in Franco *et al.* (1996), and here we just repeat the relevant parts. As the cloud is dispersed, the average gas density decreases and the newly formed cluster becomes visible. The individual HII regions merge into a single photo-ionized structure and the whole cluster now powers an extended, low density, HII region. The stellar wind bubbles now can grow to larger sizes and some of them begin to interact. As more winds collide, the region gets pressurized by interacting winds and the general structure of the gas in the cluster is now defined by this mass and energy input (Franco *et al.* 1996).

Given a total number of massive stars in the cluster, N_{OB} , and their average mass input rate, $\langle \dot{M} \rangle$, the pressure due to interacting adiabatic winds is

$$P_i \sim \frac{N_{OB} \langle \dot{M} \rangle c_i}{4\pi r_{clus}^2} \sim 10^{-8} \frac{N_2 \langle \dot{M}_6 \rangle c_{2000}}{r_{pc}^2} \text{ dyn cm}^{-2}, \quad (40)$$

where $r_{pc} = r_{clus}/1 \text{ pc}$ is the stellar group radius, $N_2 = N_{OB}/10^2$, $\langle \dot{M}_6 \rangle = \langle \dot{M} \rangle / 10^{-6} M_{\odot} \text{ yr}^{-1}$, and $c_{2000} = c_i/2000 \text{ km s}^{-1}$ is the sound speed in the interacting wind region. This is the central pressure driving the expansion of the resulting superbubble before the supernova explosion stage. For modest stellar groups with relatively extended sizes, like most OB associations in our Galaxy, the resulting pressure is only slightly above the ISM pressure (*i.e.*, for $N_2 \sim 0.5$ and $r_{pc} \sim 20$, the value is $P_i \sim 10^{-11} \text{ dyn cm}^{-2}$). For the case of rich and compact groups, as those generated in a starburst, the pressures can reach very large values. For instance, for the approximate cluster properties in starbursts described by Ho (1996), $r_{pc} \sim 3$ and $N_2 > 10$, the resulting pressures can reach values of the order of $P_1 \sim 10^{-7} \text{ dyn cm}^{-2}$, similar to those due to self-gravity in star forming cores. At these high pressures, the wind of a red giant (or supergiant) cannot expand much and the bubble reaches pressure equilibrium at a relatively small distance from the evolving star. Thus, the large mass lost during the slow red giant wind phase is concentrated in a dense circumstellar shell. Figure 4 shows the evolution of a wind-driven bubble around a $35 M_{\odot}$ star. Fig. 4a shows the wind velocity and mass-loss rate (dashed and solid lines, respectively: García-Segura, Langer & Mac Low 1996). The simulations are done only over the time spanning the red supergiant and Wolf-Rayet phases, and assume that the region is already pressurized by the main sequence winds from massive stars.

We have used the AMRA code, as described by Plewa & Różyczka (1996). During the RSG phase the wind-driven shell is located very close ($R \approx 0.04 \text{ pc}$) to the star due to a very low wind ram-pressure from the wind (Fig. 4b). Later on (Fig. 4c), the powerful WR wind pushes the shell away from the star to the maximum distance of $R \approx 0.54 \text{ pc}$. Still later, when the wind has variations, the shell adjusts its position accordingly, and reaches the distance $R \approx 0.3 \text{ pc}$ at the end of simulation (Fig. 4d). It must be stressed that the series of successive accelerations and decelerations of the shell motion during the WR phase will certainly drive flow instabilities and cause deviations from the sphericity assumed in our model. The role of these multidimensional instabilities in the evolution of the shell is currently under study (with 2-D and 3-D models), and the results will

be presented in a future communication. Regardless of the possible shell fragmentation, however, when the star explodes as a supernova, the ejecta collides with a dense circumstellar shell. This interaction generates a bright and compact supernova remnant, with a powerful photoionizing emission (*i.e.*, Terlevich *et al.* 1992; Franco *et al.* 1993; Plewa & Różyczka 1996), that may also be a very strong radio source, like SN 1993J (see Marcaide *et al.* 1995). If the shell is fragmented, the ejecta-fragment interactions will occur during a series of different time intervals, leading to a natural variability in the emission at almost any wavelength (see Cid-Fernandes *et al.* 1996). This type of interaction is also currently under investigation, and further modeling will shed more light on the evolution of SN remnants in high-pressure environs.

JF and GGS acknowledge partial support from DGAPA-UNAM grant IN105894, CONACyT grants 400354-5-4843E and 400354-5-0639PE, and a R&D Cray research grant. The work of TP was partially supported by the grant KBN 2P-304-017-07 from the Polish Committee for Scientific Research. The simulations were performed on the CRAY Y-MP of the Supercomputing Center at UNAM, and on a workstation cluster at the Max-Planck-Institut für Astrophysik.

REFERENCES

- Akeson, R. L., Carlstrom, J. E., Phillips, J. A. & Woody, D. P. 1996, ApJL, in press
- Arquilla, R. & Goldsmith, P. F. 1985, ApJ, 297, 436.
- Bergin, E., Snell, R. & Goldsmith, P. 1996, ApJ, in press
- Bisnovatyi-Kogan, G. S. & Silich, S. A. 1995, RevModPhys, 67, 661
- Bodenheimer, P. & Black, D. C. 1978, in *Protostars and Planets I*, ed. T. Gehrels, (Tucson: Univ. Arizona Press), 288
- Bregman, J. N. 1980, ApJ, 236, 577
- Brinks, E. & Bajaja, E. 1986, AA, 169, 14
- Cassen, P., Shu, F. H. & Terebey, S. 1985, in *Protostars and Planets II*, ed. D. C. Black & M. S. Matthews (Tucson: Univ. Arizona Press), 448
- Cesaroni, R., Churchwell, E., Hofner, P., Walmsley, M. & Kurtz, S. 1994, A&A, 288, 903
- Chernicaró, J., Bachiller, R. & Duvert, G. 1985, AA, 149, 273
- Chevalier, R. A. & Oegerle, W. 1979, ApJ, 227, 39
- Churchwell, E. 1990, A&AR, 2, 79
- Cid-Fernandes R., Plewa T., Różyczka M., Franco J., Tenorio-Tagle G., Terlevich R. & Miller W., 1996, MNRAS, in press
- Cioffi, D. E. & Shull, J. M. 1991, ApJ, 367, 96
- Cowie, L. L., Songaila, A. & York, D. G. 1979, ApJ, 230, 469
- Cox, D. P. 1981, ApJ, 245, 534
- Cox, D. P. 1983, ApJL, 265, L61
- Cox, D. P. & Smith, B. W. 1974, ApJL, 189, L105
- Deul, E. & Hartog, R. H. 1990, AA, 229, 362
- Díaz, R. I., Franco, J. & Shore, S. N. 1996, in preparation
- Dopita, M. 1988, *Supernova Remnants and the ISM, IAU Coll. 101*, ed. R. Roger & T. Landecker, (Cambridge Univ. Press: Cambridge), 493
- Dopita, M. A., Mathewson, D. S. & Ford, V. L. 1985, ApJ, 297, 599
- Elmegreen, B. G. 1983, MNRAS, 203, 1011
- Ferrini, F. 1992, in *Evolution of Interstellar Matter and Dynamics of Galaxies*, ed. J. Palous, W. B. Burton & P. O. Lindblad, (Cambridge: Cambridge Univ. Press), 304
- Franco, J. 1984, A&A, 137, 85
- Franco, J. 1991, in *Chemical and Dynamical Evolution of Galaxies*, ed. F. Ferrini, J. Franco & F. Matteucci, (Pisa: ETS Editrice), 506
- Franco, J. 1992, in *Star Formation in Stellar Systems*, ed. G. Tenorio-Tagle, M. Prieto & F. Sanchez, (Cambridge: Cambridge Univ. Press), 515
- Franco, J. & Cox, D. P. 1983, ApJ, 273, 243
- Franco, J., García-Segura, G. & Plewa, T. 1996, in preparation
- Franco, J., Miller, W., Cox, D., Terlevich, R., Różyczka, M. & Tenorio-Tagle, G. 1993, RMexAA, 27, 133
- Franco, J., Plewa, T. & García-Segura, G. 1996, in *Starburst Activity in Galaxies*, ed. J. Franco, R. Terlevich & A. Serrano, RMexAA (Conf. Series), in press
- Franco, J. & Shore, S. N. 1984, ApJ, 285, 813
- Franco, J., Shore, S. N. & Tenorio-Tagle, G. 1994, ApJ, 436, 795
- Franco, J., Tenorio-Tagle, G. & Bodenheimer, P. 1989, RMxAA, 18, 65
- Franco, J., Tenorio-Tagle, G. & Bodenheimer, P. 1990, ApJ, 349, 126
- García-Segura, G. & Franco, J. 1996, ApJ, in press
- García-Segura, G., Langer, N., & Mac Low, M.-M. 1996, A&A, in press

- García-Segura, G. & Mac Low, M.-M. 1995a, ApJ, 455, 145
García-Segura, G. & Mac Low, M.-M. 1995b, ApJ, 455, 160
Gerola, H. & Seiden, P. 1978, ApJ, 223, 129
Gregorio Hetem, J. C., Sanzovo, G. C. & Lepine, J. D. R. 1988, AASupp, 76, 647
Heiles, C. 1979, ApJ, 229, 533
Heiles, C. 1984, ApJS, 55, 58
Heiles, C. 1990, ApJ, 354, 483
Herbst, W. & Assousa, G. E. 1977, ApJ, 217, 473
Ho, L. 1996, in *Starburst Activity in Galaxies*, ed. J. Franco, R. Terlevich & A. Serrano, RMexAA (Conf. Series), in press
Hofner, P., Kurtz, S., Churchwell, E., Walmsley, M. & Cesaroni, R. 1996, ApJ, in press
Houck, J. C. & Bregman, J. N. 1990, ApJ, 352, 506
Hurt, R. L., Barsony, M. & Wooten, A. 1996, ApJ, in press
Kahn, F. D. 1954, BAN, 12, 187
Kurtz, S., Churchwell, E. & Wood, D. O. S. 1994, ApJS, 91, 659
Larson, R. B. 1974, FundCosmicPhys, 1, 1
Larson, R. B. 1992, in *Star Formation in Stellar Systems*, ed. G. Tenorio-Tagle, M. Prieto & F. Sanchez, (Cambridge: Cambridge Univ. Press), 125
Marcaide, J. M., Alberdi, A., Ros, E., *et al.* 1995, Science, 270, 1475
McCray, R. & Snow, T. P. Jr. 1979, ARAA, 17, 213
McKee, C. F. 1989, ApJ, 345, 782
McKee, C. F. & Ostriker, J. P. 1977, ApJ, 218, 148
Mueller, M. & Arnett, W. D. 1976, ApJ, 210, 670
Myers, P. C. 1985, in *Protostars and Planets II*, ed. D. C. Black & M. S. Matthews, (Tucson: Univ. Arizona Press), 81
Myers, P. C. & Goodman, A. A. 1988, ApJ, 326, L27
Norman, C. & Silk, J. 1980, ApJ, 238, 158
Osterbrock, D. E. 1989, *Astrophysics of Gaseous Nebulae and Active Galactic Nuclei*, (Mill Valley: Univ. Science Books)
Ostriker, J. P. & McKee, C. F. 1988, RevModPhys, 60, 1
Palous, J., Franco, J. & Tenorio-Tagle, G. 1990, AA, 227, 175
Palous, J., Tenorio-Tagle, G. & Franco, J. 1994, MNRAS, 270, 75
Plewa, T. & Różycka, M. 1996, in *Starburst Activity in Galaxies*, ed. J. Franco, R. Terlevich & A. Serrano, RMexAA (Conf. Series), in press
Reynolds, R. J. & Ogden, P. M. 1978, ApJ 224, 94
Rodríguez-Gaspar, J. A., Tenorio-Tagle, G. & Franco, J. 1995, ApJ, 451, 210
Salpeter, E. E. 1976, ApJ 229, 533
Shapiro, P. R. & Field, G. B. 1976, ApJ, 205, 762
Shore, S. N. & Ferrini, F. 1994, FundCosmicPhys, 16, 1
Silich, S., Franco, J., Palous, J. & Tenorio-Tagle, G. 1996, ApJ, 468, 000
Snell, R., Carpenter, J., Schloerrb, F. P. & Strutskie, M. 1993, in *Massive Stars: Their Lives in the Interstellar Medium*, ed. J. P. Cassinelli & E. B. Churchwell, ASP (Conf. Series) 35, 138
Steigman, G., Strittmatter, P. A. & Williams, R. E. 1975, ApJ, 198, 575
Strömgren, B. 1939, ApJ, 89, 526
Tenorio-Tagle, G. 1982, in *Regions of Recent Star Formation*, ed. R. S. Roger & P. E. Dewdney, (Dordrecht: Reidel)
Tenorio-Tagle, G. & Bodenheimer, P. 1988, ARAA, 26, 145
Terlevich, R., Tenorio-Tagle, G., Franco, J. & Melnick, J., 1992 MNRAS, 255, 713
Walmsley, M. 1995, RMexAA (Conf. Ser.), 1, 137
Weaver, R., McCray, R., Castor, J., Shapiro, P. & Moore, R. 1977, ApJ, 218, 377
Whitworth, A. 1979, MNRAS, 186, 59
Xie, T., Mundy, L. G., Vogel, S. N. & Hofner, P. 1996, ApJ, submitted
Yorke, H. W. 1986, ARAA, 24, 46